

# Fast Switching Electrochromic Display Using a Viologen-Modified ZnO Nanowire Array Electrode

X. W. Sun\* and J. X. Wang\*

*School of Electrical and Electronic Engineering, Nanyang Technological University,  
Nanyang Avenue, Singapore 639798*

*Received February 18, 2008; Revised Manuscript Received May 14, 2008*

## ABSTRACT

We report an electrochromic (EC) display using a viologen-modified ZnO nanowire array as the EC electrode. The ZnO nanowire array was grown directly on an indium tin oxide (ITO) glass by a low temperature aqueous thermal decomposition method and then modified with viologen molecules. The ZnO nanowire electrochromic device shows fast switching time (170 and 142 ms for coloration and bleaching respectively for a 1 cm<sup>2</sup> cell), high coloration efficiency (196 C<sup>-1</sup> cm<sup>2</sup>) and good stability. The improved performance of the ZnO nanowires EC device can be attributed to the large surface area and high crystalline and good electron transport properties of the ZnO nanowire array.

Electrochromic (EC) devices are capable of reversibly changing their optical properties upon charge injection and extraction induced by the external voltage. The characteristics of the EC device, such as low power consumption, high coloration efficiency, and memory effects under open circuit status, make them suitable for use in a variety of applications including EC displays,<sup>1</sup> smart windows,<sup>2</sup> and electronic papers.<sup>3</sup> Generally, there are two kinds of the EC devices: (1) coloration due to the intercalation of small ions into the thin oxide films such as WO<sub>3</sub>, NiO, and V<sub>2</sub>O<sub>5</sub>,<sup>4</sup> and (2) coloration due to reduction or oxidation of redox chromophores including some organic dye molecules. Since the time for inserting or deinserting small ions into the EC materials is relatively long (up to tens of seconds), type 1 devices are not suitable for application in displays. For type 2 devices, though, a monolayer of redox chromophore can be colored/decoupled with relatively rapid switching (several seconds); the switching time is still not sufficient for practical applications.<sup>5</sup> Recently, with increasing demand for the low cost, lightweight flat panel display with paper-like readability (electronic paper), an EC display technology based on dye-modified TiO<sub>2</sub> nanoparticle electrode was developed.<sup>6</sup> A well-known organic dye molecule, viologen, was adsorbed on the surface of a mesoporous TiO<sub>2</sub> nanoparticle film to form the EC electrode. The white background color of the TiO<sub>2</sub> nanoparticles, fast interfacial electron transfer between the TiO<sub>2</sub> nanoparticles and the viologen, and high dye loading due to the large surface area of nanoparticles render this type of EC display with much improved performance such as low

power consumption, paper-like quality, and especially fast switching time reaching several hundred milliseconds, realizing a successful business.<sup>6</sup>

On the other hand, ZnO is a wide bandgap II–VI semiconductor which has been applied in many fields such as UV lasers, field effect transistors, and transparent conductors.<sup>7</sup> The bandgap of the bulk ZnO is about 3.37 eV, which is close to that of the TiO<sub>2</sub> (3.4 eV). As a traditional transparent conductor, ZnO has excellent electron transport properties, even in ZnO nanoparticle films.<sup>8</sup> Moreover, ZnO is a cheap and environmentally friendly material. Utilization of ZnO in EC devices may further reduce the cost.

In the past few years, one-dimension (1D) nanostructures of ZnO have attracted extensive research interest. Making use of their large surface area and good electron transporting properties, new nanodevices including dye-sensitized solar cell, glucose biosensor,<sup>9</sup> and gas sensor<sup>10</sup> were fabricated. Compared with their thin-film counterparts, the nanoscale devices enable new functions, high efficiency, and enhanced performance. However, the traditional synthesis method of the ZnO nanowires (vapor phase transport, metal organic chemical vapor deposition, etc.) always requires high temperature (>500 °C), and the yield of the ZnO nanowires is relatively low, limiting the practical applications in many areas including EC field. Up to now, there is no report yet on applying ZnO nanowires in the EC devices. Meanwhile, a simple aqueous thermal decomposition method was developed by Vayssieres<sup>11</sup> in fabricating uniform and large area ZnO nanowire arrays directly on ITO transparent substrates at low temperature (<100 °C), which makes it possible to fabricate the ZnO nanowire EC device. Compared

\* Corresponding author. E-mail: exwsun@ntu.edu.sg and jxwang@cityu.edu.hk

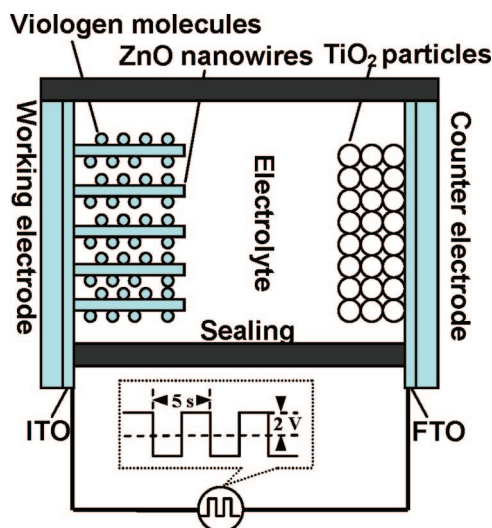


**Figure 1.** Schematics of the ZnO nanowire EC cell.

with nanoparticles, the 1D feature of ZnO nanowires renders much better electron transportation capability by providing a direct conduction path for electron transport and greatly reducing the number of grain boundaries. These unique advantages make ZnO nanowires a promising matrix electrode for EC dye molecule loading.

In this communication, we report for the first time an EC display using the viologen-modified ZnO nanowire array as the EC electrode. The large scale ZnO nanowire array was grown directly on the indium tin oxide (ITO) glass by a low temperature aqueous thermal decomposition method and modified with viologen molecules. The viologen-modified ZnO nanowire cathode shows fast switching time, high coloration efficiency, and good stability. The excellent performance of the ZnO nanowire EC display suggests a promising way to develop a low cost display technology with great commercial potential.

Figure 1 schematically shows the configuration of a ZnO nanowire array EC cell. The ZnO nanowire array was hydrothermally prepared using the procedures reported elsewhere.<sup>10</sup> In brief, ITO glass ( $2 \times 2$  cm) was first immersed in an 80 mL 5 mM zinc acetate aqueous solution with a small amount of ammonia (28%, Wako Chemicals, 0–5 mL) in a bottle with autoclavable screw cap, and then the solution was kept at 95 °C for 12 h with the solution refreshed every 3 h. Before the growth, a thin layer of ZnO film with the thickness of about 5 nm was sputtered on the ITO substrate as the seed layer. After reaction, a uniform ZnO nanowire array covering ITO glass was obtained. To fabricate the EC cell, ZnO nanowires grown at the edge of the substrate were removed using HCl (10%) leaving an area of 1 cm  $\times$  1 cm covered with a ZnO nanowire array.

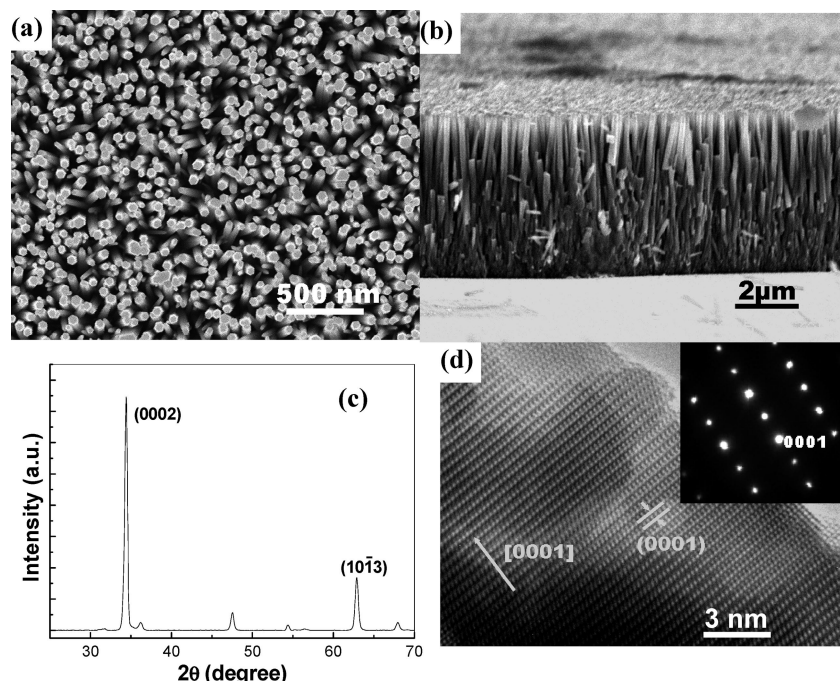
The as-grown ZnO nanowire array was first treated by oxygen plasma for 5 min and baked in an oven at 150 °C for 5 h. Then the array was immersed in a 0.02 M aqueous solution of methyl viologen for 24 h, followed by a wash with 2-propanol to remove the unattached viologen. Subsequently, the viologen-modified ZnO nanowire electrode was dried in air and stored in a vacuumed dark chamber for 24 h prior to use.

For the counter electrode, a transparent TiO<sub>2</sub> mesoporous film on F-doped tin oxide (FTO) glass was used. To fabricate this TiO<sub>2</sub> mesoporous film on FTO, we first dispersed 1 g TiO<sub>2</sub> nanoparticles (20 nm in diameter) in 5 mL deionized water with the addition of a small amount of 0.1 M acetic acid. The solution was aged at 150 °C for 12 h and then 0.5 g carbowax 1540 was added. After stirring for 8 h, the solution yielded a viscous paste, which was then spread on the FTO glass masked by a Scotch tape to yield a thin film. The film was dried in air at 80 °C and sintered at 450 °C for 1 h to obtain a transparent TiO<sub>2</sub> mesoporous film with a thickness of about 3–4  $\mu$ m. To increase the charge storage capacity of the counter electrode, a CeO<sub>2</sub> layer of 100 nm thick was deposited on the TiO<sub>2</sub> film by pulsed FCVA method.<sup>12</sup>

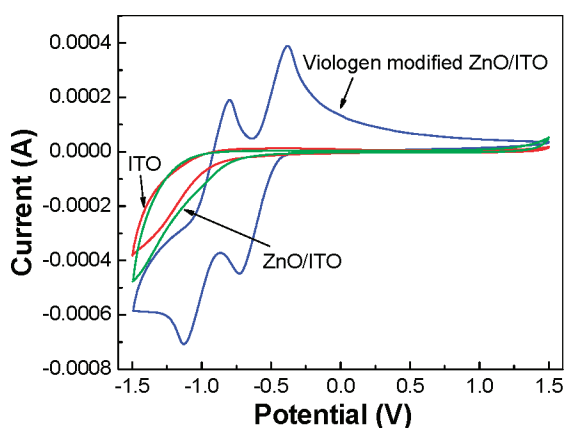
The two electrodes were separated by 100  $\mu$ m thermal-plastic Suryln spacers and bonded by epoxy. The electrolyte composed of 0.2 M LiClO<sub>4</sub> in  $\gamma$ -butyrolactone was introduced between the two electrodes by capillary action. Finally, the cell was sealed for further measurement. Since the performance of the EC cell is sensitive to oxygen, all the chemicals were bubbled with dry N<sub>2</sub> prior to the experiment.

Figure 2a,b shows the top-view and cross-section scanning electron microscopy (SEM) images, respectively, of the as-prepared ZnO nanowire array on ITO glass. It can be seen from Figure 2a that ZnO nanowires grow vertically from the substrate and form a dense array. The ZnO nanowires show a regular hexagonal cross section, and the average diameter of the ZnO nanowires is about 100 nm. The cross-section image of the ZnO nanowires array shown in Figure 2b indicates that the length of the ZnO nanowires is about 6  $\mu$ m. Figure 2c shows the XRD pattern of the working electrode. The XRD pattern was dominated by the (0002) peak, indicating the up-standing ZnO-nanowire grows along the *c* axis of the wurtzite ZnO. Figure 2d shows the HRTEM image of the ZnO nanowire. The clear fringe in the image is corresponding to the (0001) plane of ZnO, indicating single crystal quality of the ZnO nanowire. From the corresponding SAED pattern of the ZnO nanowire shown in the inset of the Figure 2d, the growth direction of the ZnO nanowires can be determined to the [0001], which is consistent with the XRD results.

To understand the oxidation and reduction behavior of the viologen-modified ZnO nanowire electrode, cyclic voltammograms (CVs) of the ZnO nanowire electrode were recorded by a CHI 660 potentiostat. The test was carried out in a standard three-electrode configuration in the solution of  $\gamma$ -butyrolactone with 0.2 M LiClO<sub>4</sub>. Figure 3 shows the CV curves obtained with a 50 mV/s scan speed for bare ITO electrode, ZnO nanowires/ITO electrode, and viologen-modified ZnO nanowires/ITO electrode, respectively. It can be seen from Figure 3 that there is no apparent redox peak for the bare ITO electrode and the ZnO nanowires/ITO electrode. However, four redox peaks are found for the viologen-modified ZnO nanowires/ITO electrode. The two peaks located at  $-0.72$  V and  $-1.12$  V (vs Ag/AgCl sat. KCl reference electrode) during the reduction scan can be assigned to the reductions that yield the singly and doubly



**Figure 2.** (a) SEM image of the ZnO nanowires array hydrothermally grown on ITO glass substrate. The diameter of the ZnO nanowires is about 100 nm. (b) Cross section of the as-prepared ZnO nanowires array; the thickness of the ZnO nanowires array is about 10  $\mu\text{m}$ . (c) XRD pattern of the ZnO nanowires array. (d) HRTEM image of the ZnO nanowires; the growth direction of the ZnO nanowire is [0001]. Inset is the SAED pattern of the ZnO nanowire.



**Figure 3.** Comparisons of the cyclic voltammograms (CVs) for bare ITO electrode, ZnO nanowires/ITO electrode, and viologen-modified ZnO nanowires/ITO electrode, respectively. The scan speed is 50 mV/s.

reduced viologen species, while the two peaks located at  $-0.8$  V and  $-0.37$  V are related to the oxidations of the singly and doubly reduced viologen, respectively.<sup>13</sup> The viologen-modified ZnO nanowire electrode is colored to blue during the reduction scan and bleached to transparent during the oxidation scan.

The response time measurement was performed by connecting the assembled ZnO nanowire EC cell to a function generator, which outputs a 0.1 Hz square wave of 2 V amplitude (i.e., 4 V peak–peak) with equal duties on the viologen-modified ZnO nanowire electrode and the counter electrode. Figure 4a shows the optical image of the as fabricated EC cell with viologen-modified ZnO nanowire electrode. The EC cell is transparent. When the ZnO

nanowire electrode was negatively biased with respect to the counter electrode, the transparent cell rapidly changed its color to deep blue (Figure 4b). Owing to the separated charges in the electrolyte and the counter electrode, the blue color can be retained for over 1 h after removal of the external voltage (Figure 4c). This so-called “memory effect” under opened circuit has great potential for applications in electronic paper. When the viologen-modified ZnO electrode was biased with a positive voltage of 2V, the cell was bleached to the original state quickly. The colored state and the bleached state of the ZnO EC cell can be switched rapidly by applying a 2V square wave (Supporting Information).

Figure 4d shows the UV–vis absorption spectra of the viologen-modified ZnO electrodes for the colored and bleached state. The spectrum of the colored cell shows an absorption peak in the visible region centered at 608 nm, while no apparent peaks are found in the spectrum of the bleached electrode. The absorbance difference  $\Delta A$  between the bleached state and the colored state at 608 nm is about 0.47 absorbance units. The apparent surface concentration of viologen on the ZnO nanowire electrode can be estimated from the followed equation:<sup>14</sup>  $\Delta A = \Gamma_R \cdot \xi_R \cdot 1000$ , where  $\Gamma_R$  is the apparent surface concentration of viologen of the electrode and  $\xi_R$  is the extinction coefficient of the viologen radical in solution, which can be taken as  $1.37 \times 10^4 \text{ M}^{-1}\text{cm}^{-1}$  at 608 nm, that is, the extinction coefficient of the methyviologen in water.<sup>15</sup> The apparent surface concentration of viologen on the ZnO nanowire electrode is calculated to be  $3.3 \times 10^{-8} \text{ mol/cm}^2$ , which is close to that of the  $\text{TiO}_2$  (5 nm) mesoporous EC electrode.<sup>6a,d</sup>

The coloration efficiency of the EC device can be defined by  $C_E(\lambda) = \Delta A(\lambda) / \Delta Q(\lambda)$ ,<sup>6e</sup> where  $\Delta Q(\lambda)$  is the correspond-



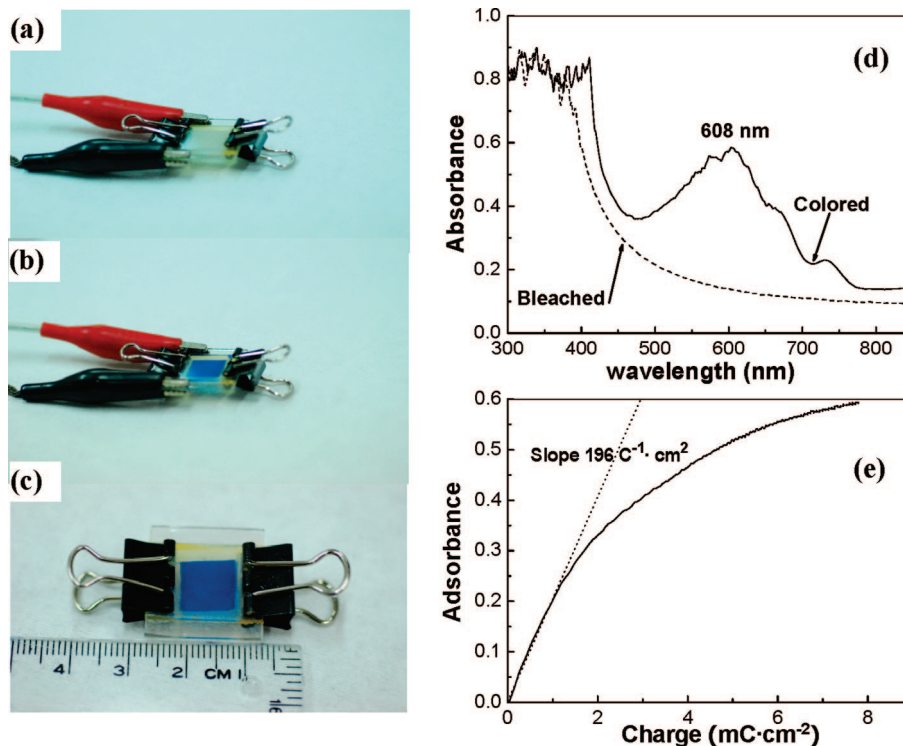


**Figure 4.** Photographs of the ZnO nanowires EC cell (a) prior to application of the external voltage, (b) after applying the external voltage, and (c) in open circuit state. (d) UV-vis absorption spectrum of the viologen-modified ZnO electrodes in colored state (solid line) and bleached state (dashed line). (e) Plot of the absorbance  $A$  versus the charge accumulated in the ZnO EC device. The coloration efficiency is  $196 \text{ C}^{-1} \text{ cm}^2$ .

ing accumulated charge for absorbance change  $\Delta A(\lambda)$ . Therefore, the coloration efficiency can be determined from the slope of the plot of the absorbance  $A$  versus the accumulated charge  $Q$ . Figure 4e shows the plot of  $A$  versus  $Q$  for the ZnO EC device. A linear relationship between the absorbance and the accumulated charge is found initially. From Figure 4e, the coloration efficiency of the ZnO chromic device is measured to be  $196 \text{ C}^{-1} \text{ cm}^2$ , which is slightly higher than that of  $\text{TiO}_2$  mesoporous film ( $170 \text{ C}^{-1} \text{ cm}^2$ ).<sup>6a</sup>

The switching time of the ZnO nanowires EC cell was studied by a reflectance measurement. The coloration time is defined as the time for the reflectance to decrease by 2/3 of the reflectance difference between the steady bleached and the colored state. The reflectance of the ZnO EC cell is high in the bleached state and low in the colored state. Correspondingly, the bleaching time is defined as the time for the reflectance to increase by 2/3 of the reflectance difference between the steady colored and the bleached state. Figure 5a shows the reflectance as a function of time for a ZnO EC cell driven by a square wave (2 V amplitude) at both the initial stage and the stage after 200 cycles. We can see that the ZnO EC device shows relatively good stability by comparing the switching curve after 200 cycles with the initial one (Figure 5a). The reflectance change is less than 10% for both colored and bleached states after 200 cycles. It is worth mentioning that the variation of the reflectance change (Figure 5a) is mainly due to improper sealing but not related to the ZnO nanowire electrode used. Taken from Figure 5a, Figure 5b shows one on/off cycle of the ZnO EC cell. We can see that the switching time of a ZnO nanowire

electrode EC cell with an active area of  $1 \times 1 \text{ cm}^2$  is 170 and 142 ms for coloration and bleaching, respectively. The coloration and bleaching time is faster compared with the  $\text{TiO}_2$  mesoporous EC devices with both coloration and bleaching time of about 250 ms for a device with an active area of  $2.5 \text{ cm}^2$ .<sup>6c</sup>

Similar to the  $\text{TiO}_2$  mesoporous EC device,<sup>6c</sup> the switching time of the ZnO EC device is also affected by the applied bias and the active area of the device. Figure 5c shows the relationship between the switching time and the applied voltage of the ZnO EC cell. The switching time reduces with an increase of applied voltage and reduces slowly with more than 2 V of bias. When the voltage is increased to the 3 V, the switching time decreases to less than 100 ms. Further increase in applied voltage, though coloration can be enhanced and switching time can be shortened, the excessive voltage (more than 3 V) applied in the EC cell will result in degradation; the cell becomes increasingly difficult to be bleached because of the desorption of the viologen molecules. The hydrothermal method can be easily scaled up. In our experiment, ZnO nanowire EC devices with various active areas ranging from  $0.1 \text{ cm}^2$  to about  $15 \text{ cm}^2$  were fabricated and their switching time was tested. Figure 5d shows the switching time as a function of the active area of the ZnO EC device. The switching time is found to increase with the increase of active area and shows almost a linear relationship with the active area. For a  $3.8 \text{ cm} \times 3.8 \text{ cm}$  ZnO nanowires EC cell, the coloration and bleaching times are increased to 1.36 and 1.33 s, respectively. The slope of the plot is measured to be  $85 \text{ ms/cm}^2$ , which may be used as a guide

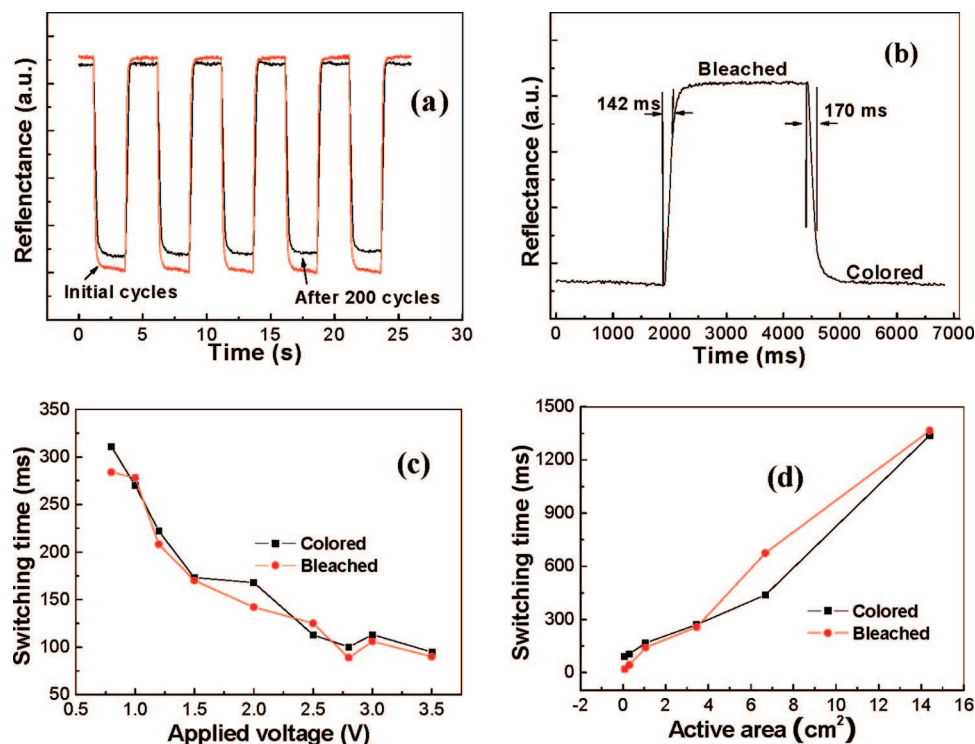


**Figure 5.** (a) Plot of the reflectance of ZnO EC cell versus time. (b) Enlarged plot of (a); the coloration time and bleached time is measured to be 170 and 142 ms, respectively. (c) Plot of the switching time versus applied voltage and (d) plot of the switching time versus active area of the ZnO EC cell.

to predict the switching time of ZnO EC device with certain dimension.

The fast switching and stable performance of the ZnO nanowire EC device can be attributed to the following: (1) the ordered ZnO nanowire array provides a porous supporting matrix for the adsorption of redox chromophore (viologen molecule in this case). For EC devices utilizing dye molecules in the electrolyte, the switching time is limited by the diffusion rate of viologen molecules to the electrode. However, for ZnO nanowire EC electrode, viologen molecules are adsorbed on the surface of the ZnO nanowires, electron communication between the ZnO nanowire surface and the adsorbed viologen molecules is direct without any scattering. As a consequence, the switching speed is greatly reduced. In addition, the 1D feature of ZnO nanowires provides many direct electrical pathways, ensuring rapid electron transportation. Furthermore, since the ZnO nanowires array is directly grown on ITO glass, the adhesion between the ZnO nanowires and the substrate is relatively better compared with the traditional mesoporous film fabricated on ITO glass by screening printing.<sup>6c</sup> Good adhesion benefits a mechanically robust device and a good electrical contact and hence a fast switching speed. Moreover, compared with the nanoparticle mesoporous film, the ZnO nanowires possess a high crystalline structure, which benefits electron transport.

It is worth mentioning that the surface area of the nanowire array is smaller than that of the nanoparticle mesoporous film, which limits the viologen loading on the ZnO nanowire array. Interestingly, our results showed that the performance of the ZnO nanowires EC device is slightly better than that

of the TiO<sub>2</sub> nanoparticle EC device. To further improve the performance of the ZnO EC device to a competitive level with the current TiO<sub>2</sub> nanoparticle EC device, we should aim for finer ZnO nanowires with larger surface area. The EC device structure needs to be improved as well. Nevertheless, the ZnO nanowire EC electrode is a promising variant of the most successful EC electrode. By further optimizing the ZnO nanowire EC electrode and cell, it is possible to develop a low cost and commercially viable EC product with fast switching.

In conclusion, we have successfully fabricated an EC display device using a ZnO nanowire array grown by aqueous thermal decomposition at low temperature. The ZnO nanowire EC cell exhibited fast switching speed (170 and 142 ms for coloration and bleaching, respectively, for a 1 cm<sup>2</sup> cell), high coloration efficiency (196 C<sup>-1</sup> cm<sup>2</sup>), and good stability. Our results demonstrate that ZnO nanowires can be a promising candidate for an EC display device, which has the potential in realizing a low cost “electronic paper”.

**Acknowledgment.** X.W.S. would like to thank C. M. Lieber of Harvard University for enlightening discussions. The sponsorships from Research Grant Manpower Fund (RGM 21/04) of Nanyang Technological University, and Science and Engineering Research Council Grant (0421010010) from Agency for Science, Technology and Research (A\*STAR), Singapore are gratefully acknowledged.

**Supporting Information Available:** Video of a ZnO nanowire electrode electrochromic display driven by a square wave with 2 V amplitude (i.e., 4 V peak-to-peak). This

material is available free of charge via the Internet at <http://pubs.acs.org>.

## References

- (1) Azens, A.; Vaivars, G.; Veszelei, M.; Kullman, L.; Granqvist, C. G. *J. Appl. Phys.* **2001**, *89*, 7885.
- (2) Ahn, K. S.; Nah, Y. C.; Cho, K. Y.; Shin, S. S.; Park, J. K.; Sung, Y. E. *Appl. Phys. Lett.* **2002**, *81*, 3930.
- (3) Corr, D.; Bach, U.; Fay, D.; Kinsella, M.; McAtamney, C.; O'Reilly, F.; Rao, S. N.; Stobie, N. *Solid State Ionics* **2003**, *165*, 315.
- (4) (a) Cheng, K. C.; Chen, F. R.; Kai, J. J. *Sol. Energy Mater. Sol. Cells* **2006**, *90*, 1156. (b) Ghicov, A.; Tsuchiya, H.; Hahn, R.; Macak, J. M.; Munoz, A. G.; Schmuki, P. *Electrochem. Commun.* **2006**, *8*, 528. (c) Azens, A.; Vaivars, G.; Veszelei, M.; Kullman, L.; Granqvist, C. G. *J. Appl. Phys.* **2001**, *89*, 7886. (d) Liao, C. C.; Chen, F. R.; Kai, J. J. *Sol. Energy Mater. Sol. Cells* **2006**, *90*, 1147.
- (5) Cinnsealach, R.; Boschloo, G.; Rao, S. N.; Fitzmaurice, D. *Sol. Energy Mater. Sol. Cells* **1998**, *55*, 215.
- (6) (a) Cinnsealach, R.; Boschloo, G.; Rao, S. N.; Fitzmaurice, D. *Sol. Energy Mater. Sol. Cells* **1999**, *57*, 125. (b) Hagfeldt, A.; Vlachopoulos, N.; Griitzel, M. *J. Electrochem. Soc.* **1994**, *141*, 7. (c) Pettersson, H.; Gruszeckia, T.; Johansson, L. H.; Edwards, M. O. M.; Hagfeldt, A.; Matuszczyk, T. *Displays* **2004**, *25*, 223. (d) Choi, S. Y.; Mamak, M.; Coombs, N.; Chopra, N.; Ozin, G. A. *Nano Lett.* **2004**, *4*, 1231. (e) Cummins, D.; Boschloo, G.; Ryan, M.; Corr, D.; Rao, S. N.; Fitzmaurice, D. *J. Phys. Chem. B* **2000**, *104*, 11449. (f) [www.ntera.com](http://www.ntera.com).
- (7) (a) Sun, X. W.; Kwok, H. S. *J. Appl. Phys.* **1999**, *86*, 408. (b) Lim, S. J.; Kwon, S. J.; Kim, H.; Park, J. S. *Appl. Phys. Lett.* **2007**, *91*, 183517. (c) Hwang, D. K.; Kang, S. H.; Lim, J. H.; Yang, E. J.; Oh, J. Y.; Yang, J. H.; Park, S. J. *Appl. Phys. Lett.* **2005**, *86*, 222101.
- (8) Roest, A. L.; Kelly, J. J.; Vanmaekelbergh, D.; Meulenkaamp, E. A. *Phys. Rev. Lett.* **2002**, *89*, 36801.
- (9) (a) Jiang, C. Y.; Sun, X. W.; Lo, G. Q.; Kwong, D. L.; Wang, J. X. *Appl. Phys. Lett.* **2007**, *90*, 263501. (b) Wang, J. X.; Sun, X. W.; Wei, A.; Lei, Y.; Cai, X. P.; Li, C. M.; Dong, Z. L. *Appl. Phys. Lett.* **2006**, *88*, 233106.
- (10) Wang, J. X.; Sun, X. W.; Yang, Y.; Huang, H.; Lee, Y. C.; Tan, O. K.; Vayssieres, L. *Nanotechnology* **2006**, *17*, 4995.
- (11) (a) Vayssieres, L. *Adv. Mater.* **2003**, *15*, 464. (b) Vayssieres, L.; Keis, K.; Lindquist, S. E.; Hagfeldt, A. *J. Phys. Chem. B* **2001**, *105*, 3350.
- (12) Tay, B. K.; Zhao, Z. W.; Chua, D. H. C. *Mater. Sci. Eng. R* **2006**, *52*, 1.
- (13) Monk, P. M. S.; Delage, F.; Vieira, S. M. C. *Electrochim. Acta* **2001**, *46*, 2195.
- (14) (a) Campus, F.; Bonhote, P.; Gratzel, M.; Heinen, S.; Walder, L. *Sol. Energy Mater. Sol. Cells* **1999**, *56*, 281. (b) Felderhoff, M.; Heinen, S.; Molisho, N.; Webersinn, S.; Walder, L. *Helv. Chim. Acta* **2000**, *83*, 181.
- (15) Wantanabe, T.; Honda, K. *J. Phys. Chem.* **1982**, *86*, 2617.
- (16) Marguerettaz, X.; O'Neill, R.; Fitzmaurice, D. *J. Am. Chem. Soc.* **1994**, *116*, 2629.

NL0804856